Viticulture extension in response to global climate change drivers - lessons from the past and future projections

Joel Guiot (guiot@cerege.fr)
CNRS
Nicolas Bernigaud
Aix-Marseille Université: Aix-Marseille Universite
Alberte Bondeau
Aix-Marseille Université: Aix-Marseille Universite
Laurent Bouby
Universite de Montpellier
Wolfgang Cramer
Aix-Marseille Universite

Research Article

Keywords: climate model emulator, Mediterranean area, viticulture, Holocene, future scenarios, forcing attribution

Posted Date: July 12th, 2022

DOI: https://doi.org/10.21203/rs.3.rs-1763994/v1

Abstract

The potential areal extent of agricultural crops is sensitive to climate change and its underlying drivers. To distinguish between the drivers of past variations in the Mediterranean viticulture since Early Antiquity and improve projections for the future, we propose an original attribution method based on an emulation of coupled climate and ecosystem models. The emulator connects the potential productivity of grapevines to global climate drivers, notably orbital parameters, solar and volcanic activities, demography and greenhouse gas concentrations. We found that variations in potential area for viticulture during the last three millennia in the Mediterranean Basin were mainly due to volcanic activity, while the effect of solar activity and orbital changes were negligible. In the future, as expected, the dominating factor is the increase in greenhouse gases, causing significantly drier conditions and thus major difficulties for viticulture in Spain and North Africa. These constraints will concern significant areas of the Southern Mediterranean Basin when global warming exceeds +2°C above pre-industrial conditions. Our experiments showed that even an intense volcanic activity comparable to that of the Samalas - sometimes considered as the starting point of the Little Ice Age at the mid 13th century - would not slow down this decline in viticulture yield in the southern margin of the Mediterranean area.

1. Introduction

Our scientific question is related to the attribution the viticulture extension changes - which has an economical role in the Mediterranean Basin since Antiquity - to any natural or anthropogenic drivers. The cultivation and domestication of the grapevine began between the 7th and 4th millennia before the common era (BCE) between the Eastern Mediterranean and Caspian areas, and spread to Egypt, the Middle East and the entire Mediterranean (Terral *et al* 2010, Bouby *et al* 2021). Introduced in the Gaul region (i.e. roughly France and surrounding regions) by Greek colonists ca. 600 BCE, around the time they settled Marseilles, viticulture was initially limited to Mediterranean Gaul (Bouby *et al* 2014). Vineyards expanded into the northern part of Gaul in the 1st century CE, where wine production developed quite considerably in the following centuries up to the Paris region, and the Rhine and Moselle valleys (Brun 2010), and even in southern England (Brown *et al* 2001). One hypothesis behind this expansion is the climate warming during the Roman Climatic Optimum (RCO) (Mccormick *et al* 2012). These climate variations are driven by global forcing variables such as solar or volcanic (Wanner *et al* 2008, Brayshaw *et al* 2010, Fuks *et al* 2017). After the RCO, the temperature decreased significantly and Gaul entered the so-called Late Antique Little Ice Age, or LALIA (536-660 CE) (Büntgen *et al* 2016). This change may have been triggered by to several large volcanic eruptions at 536, 540 and 547 CE (Sigl *et al* 2015). This assumption remains difficult to prove because of the limited historical and archaeological sources. In any case, the 500 to 900 CE period remained relatively cold with oscillating precipitation changes in the region (Reale and Dirmeyer 2000). In Europe, the following Medieval Climate Anomaly (MCA, approx. 900-1200 CE) (Luterbacher *et al* 2016) was likely of comparable intensity to the RCO. The Little Ice Age (LIA, approx. 1250-1850 CE) was a period of alpine glacier advance (Holzhauser *et al* 2005), marked again by several large volcanic eruptions, in particular that of the Samalas (Indonesia) in 1257 (Lavigne *et al* 2013).

On timescales of centuries and millennia, productivity and yield of agricultural crops are strongly affected by climate fluctuations. The nature of the change depends on external forcings and internal feedbacks of the climate system, which produce different spatial and seasonal patterns of the main variables in the atmospheric environment. The main objective of this paper is to develop an innovative solution to statistically model the impact of changing climate forcing on plant productivity over several millennia, using the grapevine (a major crop of the Mediterranean and European region) as example. We mimic a large ensemble of model simulations, using statistical relationships much faster to be computed (Kennedy and O'Hagan 2000). Based on a large range of climate states from high-resolution simulations with coupled earth system models for the last glacial period to future global warming scenarios, this approach provides be robust results and can be applied to a large range of ecosystem processes under different conditions.

The global drivers of the studied changes are anthropogenic - greenhouse gases emissions (GHG), land use and cover changes, population density, economic production - and natural - volcanic and solar activity. They are the boundary conditions of Earth System Models (ESM) (Kay *et al* 2014). The ecosystem processes are assessed using impact models (IM) coupled to these ESMs (Franklin *et al* 2016, Warszawski *et al* 2014, Frieler *et al* 2017). In most cases, coupling is offline because (i) the spatial scales of ecosystems are much finer than are those of ESMs, thus making it necessary to downscale climate simulations to the ecosystem scale; (ii) a climate simulation of a given ESM is interpreted as one realization out of a set of possibilities determined by the boundary conditions and the characteristics of the ESM, making necessary to combine ESM simulations into ensembles to be representative of the climate system; and (iii) each ESM has intrinsic biases that must be corrected before it can be used to drive the ecosystem model. We use the ecosystem model BIOME4 which takes all ecosystem-related variables into account, notably rainfall, temperature with their full seasonal cycle, and also soil moisture as an internal state variable.

Even if human innovation and colonization were also responsible for the expansion of viticulture, the climate must be suitable for grape cultivation and thus remains a control variable. As soon as the climate changes to worse conditions for wine growth, it becomes a driver of a decline in viticulture. Such fluctuations are particularly noticeable near the Northern range limit of wine growth during several periods.

Although we focus our viticultural analysis on the Gaul region, we need to enlarge the area to the entire Mediterranean and European surrounding region to robustly capture the relationships between global drivers and viticulture extension. For the same reason, we use a large diversity of time slices of the past (Last Glacial Maximum, Mid-Holocene, last millennium) and of the future up to 2100 according to several scenarios. The widely diverse situations used for calibration made it possible to produce a robust emulator that was effective for extrapolating a wide range of past and future climate states.

2. Material And Method

Our method is summarized in Fig. 1, and the different steps are explained in details in Supplementary Material. Global forcings are the inputs of low-resolution Earth system models (ESMs). The first step in the emulator procedure involves adapting the output fields to a common high-resolution grid using statistical downscaling. The second step involves applying the vegetation model BIOME4 to the high-resolution fields to calculate ecosystem variables (bioclimate or net

primary productivity, Table S1). Steps 1 and 2 are repeated for each ESM. Step 3 is the calibration of the emulator, that is, the calculation of a spatial regression between the forcing and the ecosystem variables. Step 4 involves the application of the emulator to the forcings of new time slices or future scenarios. During this step, the annual temperature and precipitation results for the past time slice were compared to paleodata to refine the volcanic and solar activity impacts. This process is known as data assimilation. The last step, which is not shown in the figure, is the independent validation of the emulator using tree-ring data.

2.1 Forcing and ESM data

Climate forcing or drivers are perturbations imposed on the Earth's energy balance. They are mainly:

(i) Orbital parameters: eccentricity and obliquity of the ecliptic, solar longitude at the perihelion (omega); they drive the orbit of the Earth and have time lengths above thousands of years (Berger and Loutre 1991); they had a major impact on the Earth climate from the last glacial period to the present interglacial period (the Holocene); the values of the last millennium were linearly interpolated between the values at 1000 yr BP and the present values. Those of the 21st century were set to the present values, as this time period is short according to the time characteristics of the orbital forcing.

(ii) Greenhouse gas concentration (GHG): carbon dioxide (CO_2), methane (CH_4) and nitrous oxide (N_2O); the effect of these GHG has been significant from the glacial to interglacial periods and has a major effect for the current century (see suppl. mat. S1).

(iii) The world population values taken from the Hyde 3.1 database for the past periods from (Klein Goldewijk *et al* 2011) and for the future periods from (van Vuuren *et al* 2011). The population varied from less than 2 10^6 at the LGM (which is in fact the value at 10 ka BP in Hyde3.1) to 7 10^9 in 2010 and is projected to be between 9 10^9 and 12.3 10^9 in 2100 according to the scenario.

(iv) Volcano activity represented by the effective aerosol radius deduced from the aerosol optical depth from ice core sulfate records from both polar regions for the last millennium (Crowley and Unterman 2013) (Fig. S1). Its value is 0.2 when there is no eruption. The maximum value (0.8) was found in 1258, the year after the Samalas eruption (Lavigne *et al* 2013). The 21ka, 6ka and future values were set to the pre-industrial values.

(v) Solar activity is inferred from ^{14}C records, the proxy of the total solar irradiance (TSI) (Muscheler *et al* 2007) for the last millennium, and varies from 0 to 1200 MeV (Fig. S1). The 21ka, 6ka and future values were set to the pre-industrial values.

2.2 Data used for past and future scenarios

We used our emulator to analyze the response of key ecosystem variables to global forcing. We focused on past periods that were marked by important climate and societal changes (Table 1). The present time slice was defined by the mean values for the 1961-1990 period. For the future, instead of using time slices, we defined the scenarios according to the global temperature signal simulated in the different models, using the relationship between global warming and CO_2 concentration (Guiot and Cramer 2016):

(i) The +1.5°C global warming recommended by the Paris Agreement is reached with a CO_2 concentration of 440 ppm; Fig. S2 shows that the average model simulation reaches this value under scenario RCP2.6 in approximately 2040.

(ii) The +2°C global warming is reached with a CO_2 concentration of 480 ppm and is reached under scenario RCP4.5 in approximately 2050 (Fig. S2).

(iii) The +3°C global warming is reached with a CO_2 concentration of 600 ppm and is reached under scenario RCP8.5 in approximately 2060 (Fig. S2).

(iv) The +5°C global warming is reached with a CO_2 concentration of 900 ppm and is reached under scenario RCP8.5 in about 2100 (Fig. S2);

We obtained the corresponding CH_4 and N_2O concentrations and population sizes from the boundary condition database of CMIP5. The other forcings are set to the present values.

Following Giorgi and Lionello (2008), the study area was divided into nine grid boxes (Fig. 2). We added a 10th box corresponding to the Gallia Narbonensis province (south of France), the key area for the introduction of viticulture in Gaul.

We also considered two other scenarios, based on boundary conditions of +5°C except for volcanic and solar activity. The idea is to assess whether volcanic and solar conditions typical of the Little Ice Age can moderate the effect of the strong increase in GHG concentrations. The first additional scenario (labeled +5CV+) was assigned very substantial volcanic activity (0.8), the highest value in the last millennium, and low solar activity (i.e. 100). In contrast, the second additional scenario (labeled +5CV-) was assigned low volcanic activity (0.1) and high solar activity (700), corresponding to those of the MCA. The forcing values are listed in Table 2.

2.3 Downscaling and vegetation model

We want to establish a bridge between global drivers and ecosystem variables through an ESM and the ecosystem model. It is based on a common 0.5° grid using a statistical downscaling technique (details in the Suppl. Mat. S2). The ecosystem model is coupled offline to downscaled climate outputs, and provide indications on land vegetation structure and productivity. Here, we used a process-based equilibrium vegetation model, BIOME4 (Kaplan *et al* 2002), which has been successfully applied to similar questions before (Guiot and Cramer 2016) (details in the Suppl. Mat. S3). While a wide range of climate simulations are necessary to ensure robust calibration, the use of a single ecosystem model is required to ensure that the same ecosystem variables are calculated for all simulations.

2.4 Emulator calibration

The numerous model outputs available in the CMIP and PMIP databases (suppl. mat. Table S2) are used to calibrate robust statistical approximations of coupled ESMs and BIOME4, called emulator (Kennedy and O'Hagan 2000). Various emulators are used in climate science (Tran *et al* 2016, Zhu *et al* 2015, Rougier and Goldstein 2014, Castruccio *et al* 2014), including paleoclimatic conditions (Strassmann and Joos 2018, Joos *et al* 1996, Bounceur *et al* 2015). Our approach is the first ESM-independent emulator because it is calibrated using a large set of model simulations under very different scenarios. The calibration is based on a geographically weighted regression (Brunsdon *et al* 1998), where the ecosystem variables are expressed as functions of the global forcing variables (details in the Suppl. Mat. S4).

2.5 Paleodata assimilation

The emulator was calibrated using virtual data. To bring it closer to the real world, we used proxy-based climate reconstructions to constrain some parameters of the emulator. These parameters are related to the impact of the global forcings. The GHG concentrations, orbital parameters and population sizes are relatively well known. There are more uncertainties regarding the volcanic and solar activity impacts, which are then considered as the parameters to be optimized to better fit paleoclimate reconstructions. This technique is called data assimilation (see suppl. mat. S5). To drive the assimilation, we used the annual temperature and precipitation variables for the time slices defined in Table 1. The main quantitative paleoclimatic information was obtained from Guiot and Kaniewski (2015) with additional qualitative information found in various studies (as explained in Table 1). The assimilation was based on the 10 boxes defined in Fig. 2.

3. Results

3.1 Paleodata assimilation

The parameters that will be optimized using temperature and precipitation data, are: (i) input volcanic activity, (ii) input solar activity, (iii) a possible bias for the temperature (δT) and (iv) for the precipitation (δP), (v) the standard error of temperature (σT) and (vi) precipitation (σP).From the posterior distributions (Table 3), it appears that the volcanic activity impacts were the strongest during the cold periods (2500, 1300, 700 and 200 yr BP) and rather weak during the dry periods (4200 and 3200 yr BP) and warm periods (2000 and 1000 yr BP). The confidence intervals do not overlap so that these differences are significant. For the present slice, volcanic and solar activities have no significant impact, as it is expected that the warming is explained by increased GHG concentration (not used for constraining the assimilation). The impact of solar activity is not clear, as there is no significant difference between cold and warm periods or between the dry and wet periods. The temperature bias (δT independent of the spatial variability) is estimated to be between 0.6 and 1.6°C for the periods between 2500 and 200 yr BP and is not significantly different from zero for the dry periods and the present. The δP estimates were not significant for any time period. Fig. S4 presents the overall correlations between the emulator outputs and the proxy-based reconstructions. The temperature was particularly well simulated by the emulator with a squared correlation (R^2) of 0.75. As expected precipitation is less well simulated with an R^2 of 0.28, which is nevertheless significant, with a significant underestimation of the large (negative or positive) anomalies.

3.3 Emulator application to past and future scenarios

This assimilation process was applied to simulate the annual temperature and precipitation for the ten boxes in the 13 time slices/scenarios. The spatial patterns of the reconstructions and simulations are consistent (Fig. 3). Therefore, global forcing variables can drive not only the mean climate evolution but also the spatial patterns reconstructed by the proxy data in the Mediterranean. Volcanic activity seems to be the main driver for the cold periods of the Iron Age (2500 yr BP), the LALIA (1300 yr BP), the LIA (700, 200 yr BP), and for the warm periods of the RCO (2000 yr BP) and MCA (1000 yr BP). The main driver of the present warming and drying (Present time in Fig. 3) is GHG forcing. For the 4200 yr BP and 3200 yr BP periods, the volcanic and solar activity drivers do not seem to be plausible explanations for the droughts, at least according to our emulator.

Future projections (Fig. 4) show general warming for the four scenarios (+1.5C, +2C, +3C, +5C) particularly strong for +3C and +5C scenarios. The local warming is less strong in the areas influenced by the Atlantic Ocean (France and the Iberian Peninsula). For precipitation, we simulated a weak signal for +1.5C and +2C with drier and wetter zones, but the signal became clearer for +3C and +5C (all the symbols are triangles, i.e. negative). Combined with the warming, it is undeniable that water stress will increase considerably with +3C and +5C temperatures.

To answer the question of whether volcanic activity can mitigate the impact of high GHG emissions, fig. 4 shows that the temperature distributions of +5CV+ and 5CV- are quite similar, meaning that the cooling effect of volcanoes is low in a large GHG emission scenario. The precipitation distributions of +5CV+ and 5CV- were similar in the western Mediterranean, and +5CV+ produced slightly higher precipitation anomalies than +5CV- in the eastern Mediterranean.

3.4 Independent validation

Additional independent validation was completed through comparisons with a tree-ring-based reconstruction of the Palmer Drought Severity Index (PDSI) (Cook *et al* 2015) for the last two millennia, when tree-ring data are available. The PDSI reflects the spring-summer soil moisture conditions. We compared this variable with the reconstruction of the E/PE (ratio of actual to potential evapotranspiration in %) variable provided by BIOME4 in the previous steps. E/PE is a moisture index which is equal to zero when the soil is fully dry and 100 when it is fully wet. The range of the PDSI index is usually between -6 and 6 units. Considering that both indices are slightly different, a visual comparison shows pretty good agreement (Fig. 5).

3.5 Evolution of viticulture from the Bronze Age to the end of the 21st century

We subsequently applied our emulator to the question of how viticulture has evolved in the Mediterranean region and in response to which climatic stimuli and global forcing. Numerous bioclimate indices have been published to delimit viticultural zones in the world (Tonietto and Carbonneau 2004, Santos *et al* 2012, Howell 2001). Among them cite (1) the sum of degree-days above 10°C during the growing season or the heliothermal index of Huglin (HI), (2) the number of days with a minimum temperature below -17°C which is very important for the grapes growing in continental climates, (3) the minimum temperature of September (cool night index CI) important for the ripening, (4) the sum of the product of monthly temperature and precipitation for the growing season (Hyl), and (5) the drought stress index (DI) related to the potential water balance of the soil during the growing season. Malheiro et al. (2010) have proposed a composite index (CompI) calculated based on the ratio of years simultaneously satisfying four criteria (HI>1400, DI>-100, Hyl<5100 and Tmin >-17°C). Some of the climate variables needed for these indices were not available from the BIOME4 outputs. However, other BIOME4 variables, such as those associated with the net primary production of plant types are very interesting because they include the CO_2 effect on photosynthesis. Considering only rainfed viticulture, we propose the following index VI:

$$VI = (1 - I_{NPPtrop}) \cdot I_{NPP} \cdot I_{Pann} \cdot I_{MTWA} \cdot I_{MTCO} \cdot I_{\alpha}$$

Where each of these factors denoted I_x follows this function:

$$I_x = 0 \quad for \quad x < x_{min},$$

$$I_x = 1 \quad for \quad x > x_{max},$$

and

$$I_x = \frac{x - xmin}{(xmax - xmin)} \quad for \quad x_{min} < x < x_{max}$$

and x=NPP_{trop}, the net primary production of tropical plants with interval [x_{min}, x_{max}] equal to [0, 10 kg C m^{-2}]; x=NPP, the total ecosystem net primary production with interval = [500, 1000 kg C m^{-2}]; x=P_{ann}, the total annual precipitation with interval = [400, 800 mm]; x=MTWA, the mean temperature of the warmest month with interval = [18, 23°C]; x=MTCO, the mean temperature of the coldest month with interval [3, 12°C]; x=, the actual to potential evapotranspiration ratio with interval = [30, 60%]. The VI index combines the total ecosystem productivity of a viticultural system with a few key bioclimatic variables. All except those related to NPP_{trop} assume that the vine growth is limited only by their lower values and not by their higher values. Because there is no possible viticulture in the tropics (where temperature is not cold enough for an appropriate dormancy), 1-$I_{NPPtrop}$ is limited by its upper value.

Applied to the mean climate of 1980-2009, VI approximately reproduces the area in Europe where viticulture is present (Fraga *et al* 2013) (Fig. 6). As shown in Fig. 6a, the existing wine sites range from 35°N to 52°N. In Fig. 6b, the simulations give approximately the same limits with an optimum at approximately 42°N, with some exceptions in the Alpine and Balkan regions, which are likely too continental to pass the MTCO criterion. Considering that this criterion is much dependent on local factors such as valleys, slopes, and soil, which are not accounted for in our analysis, we consider that this index adequately represents the macroclimate of potential vine distribution in Europe and the Mediterranean region.

The variables needed for the viticulture equation (1) are provided by the emulator for all time slices studied in the past time slices and for future scenarios. As shown by fig. 7, we modify the global forcings according the values of Table 3 for the past and Table 2 for the future. We so obtain simulated maps of the viticulture extension.

Fig. 8 shows that during the dry time slices of 4200 and 3200 yr BP, the suitable areas were located between 34°N and 46°N latitudes. During the cold periods (2500, 1300, 700, and 200 yr BP), they occupied approximately the same zone between 34°N and 47°N. During the warmer periods (2000 and 1000 yr BP), the southern limit did not change much, but the northern limit reached 49°N, implying that most of Gaul was suitable for viticulture, as already shown by (Bernigaud *et al* 2021). The present map is warmer than the pre-industrial period (200 yr BP slice), which suggests that viticulture is now at its maximum potential extension in four thousand years, up to 51°N. Because of the drier conditions, the southern limit has shifted from 34°N to 35°N. Note that these variations only depend on climate changes, and that we do not consider the type of soils.

In the future projections, the northern extension of potential viticulture should shift from 51°N (+1.5C scenario) to 53°N (+3C scenario), and even more than 55°N (for the +5C scenario). This would allow viticulture to be possible up to Central England, but it would regress in the south due to higher water stress. In the Iberian Peninsula, only the Atlantic coast should be suitable for cultivating wine grapes, unless significant irrigation. These projected unfavourable conditions were confirmed by (Fraga *et al* 2013) based on other viticulture indices. The 5CV+ and 5CV- scenarios appear quite similar to the 5C scenario, indicating that the effect of high or low volcanic activities should have a weak effect on the potential distribution of the viticulture in comparison to a strong GHG forcing.

The results are summarized in Fig. 9. In the past, only the warm regions of the southern band (29-37°N) had a suitable wine-growing area equivalent to the present. The central geographical band (37-44°N) and the northern one (44-48°N) underwent sudden changes in the viticulture area, first from the cool Iron Age (2500 yr BP) to the RCO (2000 yr BP), and later from the end of the LIA (200 yr BP) to the present. The cold periods are all characterized by a decline in viticulture at latitudes above 37°N. For the future projections, northward displacements are likely to be drastic from +3°C global warming. Viticulture potential will likely disappear from North Africa and is set to decrease drastically in the Iberian Peninsula. In contrast, potential productive areas will likely expand at latitudes above 50°N, in the Balkans and in the Alps (considering that local climates already enable grape cultivation in some areas with particularly favourable local climates).

For the two additional scenarios of high emissions combined with extreme volcanic and solar activities, the question is whether an entirely hypothetical set of strong volcanic events could slow down the decline in viticulture in the south. The answer is slightly positive for Spain, Italy, Greece and Turkey (green curve increases for +5CV+ and decreases for +5CV-), but it is negative in North Africa and the Levant (red curve) because the water stress should remain too substantial. The effect is also positive in the northern band and Turkey (the blue and cyan curves increase for +5CV+ and decrease for +5CV-). In all the cases, the effect was clearly too small to compensate for the GHG effect.

4. Discussion

In this study, we demonstrate the efficiency of a statistical emulator for multiple ESMs, calibrated over a large range of forcing and climate states to link the production of a regionally important crop to global climate forcing variables. There are two main innovations: (i) past climate simulations are used together with future ones to calibrate a robust emulator, (ii) this emulator, based on multiple ESMs, is independent of any single model because it captures what is common among all the models used. Our approach ensures that the emulator is sufficiently robust to work in very different climate states compared to the present one. Similar approaches have already been used to analyse paleoclimatic data (Crucifix 2012, Joos *et al* 1996), and to emulate a climate-vegetation system (Foley *et al* 2015), but this study is the first to use an ensemble of climate models, along with several forcing variables provided by past, present and future states, to project vegetation conditions from global climate drivers. Five points are now discussed:

1) Our approach shows that the major climatic variations of the last millennia in the Mediterranean Basin can be attributed to volcanic activity, whereas the effects of solar activity were negligible. The effects of volcanic and solar activities have been largely debated, as the reconstruction of temperatures in the last millennium from tree rings has often shown less significant cooling than the model simulations (Mann *et al* 2012). A more recent tree-based reconstruction (Stoffel *et al* 2015) showed substantial summer cooling after the Samalas eruptions in 1257, and also Tambora in 1816, but less than what climate models simulated. Luterbacher et al. (2016) showed that solar activity had a relatively weak influence on the European summer temperatures. Thus, our results are in line with the state-of-the-art in the scientific literature.

2) The effect of this volcanic forcing has a clear spatial pattern across the Mediterranean basin. From 2500 yr BP to the present, temperature variations were more significant in the north and in the west than in the southeast (Fig. 3). (Fischer *et al* 2007) found that northern and western Europe were the coldest and driest areas after an eruption. They also found that southern Europe, North Africa and the Levant have experienced milder and wetter weather than at present. Part of this pattern might be due to regional feedbacks of vegetation on the climate. Some climate model simulations have shown (Reale and Dirmeyer 2000) that wetter vegetation during the RCO may have induced a northward shift of the intertropical convergence zone during the summer over the African continent with an increase of moisture in North Africa and Iberia, and a decrease in the central Mediterranean (Reale and Shukla 2000). In the future, the southeast should be relatively less dry and warmer than the northwest especially in summer, which is consistent with our results (Fig. 3) (Giorgi and Lionello 2008).

3) Our simulations of climate change on viticulture are mostly concerned with larger-scale regional production systems since they would require near-full-time engagement of winegrowers with high certainty of production every year, sufficient for speculative trade. For smaller domains and local consumption, it may have also been possible to produce wine under degraded or unstable weather conditions. For example, in England, viticulture continued to be practiced on land owned by the church, even as risks increased due to a wetter climate, with cooler summers and milder winters (Clout 2013). In most wine regions in western Europe, and particularly in France, the grape harvest dates were advanced after the LIA and particularly after the 1940s (Le Roy Ladurie *et al* 2006). For example, from 1945 to the beginning of the 21st century, in Chateauneuf du Pape (Southern Rhone Valley, France) the harvest date advanced on average from October 1 to September 11 (Ganichot 2002). This change is related to summer warming, but factors related to wine quality, agricultural practices and alcohol content regulation may induce a bias in the interpretation (de Cortázar-Atauri *et al* 2010). In the Languedoc region, the potential alcohol content has increased by two degrees from 1984 to 2013 (van Leeuwen and Darriet 2016). Even if the alcohol content does not exactly reflect the grape yields, earlier harvest dates with a higher sugar content are clearly related to improved conditions of grape cultivation since the LIA which is also related to increased productivity. Another climate-sensitive symbol of Mediterranean agriculture is the olive trees. (Moriondo *et al* 2013) found three characteristic periods in olive-growing, namely: the RCO (300 BCE to 400 CE) and the MCA (900 CE to 1200 CE) during which olive-growing areas expanded northward, and the LIA (1400 CE to 1900 CE) during which a contraction was reported. This is consistent with the variations in viticulture.

4) Major difficulties are forecast for 21st century viticulture in Spain and North Africa. These are particularly important for global warming levels of +3°C and more. (Caffarra and Eccel 2011) showed that the projected warming should make some mountain sites at approximately 1000 m climatically suitable for viticulture before the end of this century. The MCA limit will certainly be passed. However, other factors could become limiting, such as excessively mild winters that enable pest attacks and infections, lack of expertise in vine growing and wine making, and products that are more expensive than the current Mediterranean wines (Clout 2013). Another limitation is extreme events. More frequent and more intense heatwaves will no longer be favourable to viticulture at the present southern Mediterranean limit of its niche. These factors are not considered in our approach.

5) It is not very likely that intense volcanic activity could slow down this decline, because (despite of the many other negative consequences of such events) the beneficial climatic effects of this activity would be highest in regions with increased wine growing potential under global warming (Turkey, northern Europe, the Alps, and the Balkans) and negligible in North Africa. IPCC has assessed the literature concerning the question of whether volcanic eruptions could be analogous for geoengineering proposals for climate mitigation (Myhre *et al* 2013). Independent of the side effects of geoengineering, our results show that very strong volcanic activity, even when accompanied by low solar activity, should not have any significant effects on viticulture in comparison to the radiative forcing from anthropogenic GHG emissions.

5. Conclusion

We demonstrated the efficiency of a statistical emulator based on multiple Earth System models and calibrated over a large range of forcing and climate states to link the production of a regionally important crop (grapes) to global climate forcing variables. Using it on past time slices, we showed that volcanic activity is a good predictor of the past temperature variations in the Mediterranean Basin and consequently of the viticulture productivity. During the warm phases of the historical times (The Roman Climate Optimum and the Medieval Climate Anomaly), characterized by a low volcanic activity, the viticulture area has shifted northward by 2° latitude (47°N to 49°N). This historical limit has already passed at the present time as it has already shifted to 51°N and with a global warming of +3°C, it should pass the 53°N limit. Even, if in the past North Africa and Spain never had real difficulties in cultivating grapes, this

production would become impossible with a global warming of +3°C or more, except on the Atlantic margin. Moreover, our sensitivity experiments show that even an intense volcanic activity is not sufficient to stop this decline.

Statements And Declarations

Funding This work has been funded by the Excellence Initiative of Aix-Marseille University A*MIDEX, a French “Investissements d’Avenir” programme (project RDMED) and the Labex OT-Med project (project ANR-11- LABEX-0061).

Financial interests: all the authors *declare they have no financial interests*

Conflict of interest: The authors have declared that no competing interests exist.

Open access All data, codes, and materials used in the analyses are available at https://github.com/douane7/C5P3_B4_emul.git.

Author contribution

All authors contributed to discussions to prepare the manuscript. Material preparation, data collection and analysis were performed by Joel Guiot. The first draft of the manuscript was written by Joel Guiot and all authors commented on previous versions of the manuscript. All authors read and approved the final manuscript.

Acknowledgements Charles La Via edited the English.

References

1. Berger A and Loutre M F 1991 Insolation values for the climate of the last 10,000,000 years *Quat. Sci. Rev.* **10** 297–317
2. Bernigaud N, Bondeau A and Guiot J 2021 Understanding the development of viticulture in Roman Gaul during and after the Roman climate optimum: The contribution of spatial analysis and agro-ecosystem modeling *J. Archaeol. Sci. Reports* **38** 1–9
3. Bouby L, Marinval P and Terral J-F 2014 From secondary to speculative Productlon? the Protohistory history of viticulture in Southern France *Plants and People: choices and diversity through time* ed A Chevalier, E Marinova and L P Chocarro (London & Philadelphia: Oxbow Book) pp 175–81
4. Bouby L, Wales N, Jalabadze M, Rusishvili N, Bonhomme V, Ramos-Madrigal J, Evin A, Ivorra S, Lacombe T, Pagnoux C, Boaretto E, Gilbert M T P, Bacilieri R, Lordkipanidze D and Maghradze D 2021 Tracking the history of grape cultivation in Georgia combining geometric morphometrics and ancient DNA *Veg. Hist. Archaeobot.* **30** 63–76 Online: https://doi.org/10.1007/s00334-020-00803-0
5. Bounceur N, Crucifix M and Wilkinson R D 2015 Global sensitivity analysis of the climate-vegetation system to astronomical forcing: An emulator-based approach *Earth Syst. Dyn.* **6** 205–24
6. Brayshaw D J, Hoskins B and Black E 2010 Some physical drivers of changes in the winter storm tracks over the North Atlantic and Mediterranean during the Holocene. *Philos. Trans. A. Math. Phys. Eng. Sci.* **368** 5185–223 Online: http://rsta.royalsocietypublishing.org/content/368/1931/5185%5Cnhttp://rsta.royalsocietypublishing.org.ezproxy1.lib.asu.edu/content/368/1931/5185.s
7. Brown A G, Meadows I, Turner S D and Mattingley D 2001 Roman vineyards in Britain: stratigraphic and palynological data from Wollaston in the Nene Valley, England. *Antiquity* **75** 745–57 Online: https://eprints.soton.ac.uk/55242/
8. Brun J-P 2010 15. Viticulture et oléiculture en Gaule *Comment les Gaules devinrent romaines* Hors collection Sciences Humaines ed Pierre Ouzoulias (Paris: La Découverte) pp 231–53
9. Brunsdon C, Fotheringham S and Charlton M 1998 Geographically weighted regression - Modelling spatial non-stationarity *J. R. Stat. Soc. Ser. D Stat.* **47** 431–43
10. Büntgen U, Myglan V S, Ljungqvist F C, Mccormick M, Cosmo N Di, Sigl M, Jungclaus J, Wagner S, Krusic P J, Esper J, Kaplan J O, Vaan M A C De, Luterbacher J, Wacker L and Tegel W 2016 Cooling and societal change during the Late Antique Little Ice Age from 536 to around 660 AD *Nat. Geosci.*
11. Caffarra A and Eccel E 2011 Projecting the impacts of climate change on the phenology of grapevine in a mountain area *Aust. J. Grape Wine Res.* **17** 52–61
12. Castruccio S, Mclnerney D J, Stein M L, Crouch F L, Jacob R L and Moyer E J 2014 Statistical emulation of climate model projections based on precomputed GCM runs *J. Clim.* **27** 1829–44
13. Clout H 2013 An Overview of the Fluctuating Fortunes of Viticulture in England and Wales *EchoGeo* **23** Online: http://journals.openedition.org/echogeo/13333
14. Cook E R, Seager R, Kushnir Y, Briffa K R, Büntgen U, Frank D, Krusic P J, Tegel W, Schrier G Vander, Andreu-Hayles L, Baillie M, Baittinger C, Bleicher N, Bonde N, Brown D, Carrer M, Cooper R, Eùfar K, DIttmar C, Esper J, Griggs C, Gunnarson B, Günther B, Gutierrez E, Haneca K, Helama S, Herzig F, Heussner K U, Hofmann J, Janda P, Kontic R, Köse N, Kyncl T, Levaniè T, Linderholm H, Manning S, Melvin T M, Miles D, Neuwirth B, Nicolussi K, Nola P, Panayotov M, Popa I, Rothe A, Seftigen K, Seim A, Svarva H, Svoboda M, Thun T, Timonen M, Touchan R, Trotsiuk V, Trouet V, Walder F, Wany T, Wilson R and Zang C 2015 Old World megadroughts and pluvials during the Common Era *Sci. Adv.* **1** 37 Online: http://advances.sciencemag.org/
15. de Cortázar-Atauri I G, Daux V, Garnier E, Yiou P, Viovy N, Seguin B, Boursiquot J M, Parker A K, van Leeuwen C and Chuine I 2010 Climate reconstructions from grape harvest dates: Methodology and uncertainties *Holocene* **20** 599–608
16. Crowley T J and Unterman M B 2013 Technical details concerning development of a 1200 yr proxy index for global volcanism *Earth Syst. Sci. Data* **5** 187–97 Online: http://dx.doi.org/10.5194/essd-5-187-2013

17. Crucifix M 2012 Traditional and novel approaches to palaeoclimate modelling *Quat. Sci. Rev.* **57** 1–16
18. Fischer E a., Luterbacher J, Zorita E, Tett S F B, Casty C and Wanner H 2007 European climate response to tropical volcanic eruptions over the last half millennium *Geophys. Res. Lett.* **34** 1–6
19. Foley A M, Holden P B, Edwards N R, Mercure J-F, Salas P, Pollitt H and Chewpreecha U 2015 Climate model emulation in an integrated assessment framework: a case study for mitigation policies in the electricity sector *Earth Syst. Dyn. Discuss.* **6** 1277–308 Online: http://www.earth-syst-dynam-discuss.net/6/1277/2015/
20. Fraga H, Malheiro A C, Moutinho-Pereira J and Santos J A 2013 Future scenarios for viticultural zoning in Europe: Ensemble projections and uncertainties *Int. J. Biometeorol.* **57** 909–25
21. Franklin J, Serra-Diaz J M, Syphard A D and Regan H M 2016 Global change and terrestrial plant community dynamics *Proc. Natl. Acad. Sci. U. S. A.* **113** 3725–34
22. Frieler K, Lange S, Piontek F, Reyer C P O, Schewe J, Warszawski L, Zhao F, Chini L, Denvil S, Emanuel K, Geiger T, Halladay K, Hurtt G, Mengel M, Murakami D, Ostberg S, Popp A and Riva R 2017 Assessing the impacts of 1 . 5 ∘ C global warming – simulation protocol of the Inter-Sectoral Impact Model Intercomparison Project (ISIMIP2b) *Geosci. Model Dev.* **10** 4321–45 Online: https://doi.org/10.5194/gmd-10-4321-2017
23. Fuks D, Ackermann O, Ayalon A, Bar-Matthews M, Bar-Oz G, Levi Y, Maeir A M, Weiss E, Zilberman T and Safrai Z 2017 Dust clouds, climate change and coins: consiliences of palaeoclimate and economy in the Late Antique southern Levant *Levant* **49** 205–23 Online: https://doi.org/10.1080/00758914.2017.1379181
24. Ganichot B 2002 Évolution de la date des vendanges dans les Côtes du Rhône méridionales *Rencontres rhodaniennes* ed I Rhodanien (Orange) pp 38–41
25. Giorgi F and Lionello P 2008 Climate change projections for the Mediterranean region *Glob. Planet. Change* **63** 90–104
26. Guiot J and Cramer W 2016 Climate change: The 2015 Paris Agreement thresholds and Mediterranean basin ecosystems *Science (80-.).* **354** 4528–32
27. Guiot J and Kaniewski D 2015 The Mediterranean Basin and Southern Europe in a warmer world: what can we learn from the past? *Front. Earth Sci.* **3** Online: http://www.frontiersin.org/quaternary_science,_geomorphology_and_paleoenvironment/10.3389/feart.2015.00028/abstract
28. Holzhauser H, Magny M and Zumbuhl H J 2005 Glacier and lake-level variations in west-central Europe over the last 3500 years *HOLOCENE* **15** 789–801
29. Howell S G 2001 Sustainable Grape Productivity and the Growth-Yield Relationship *Am. J. Enol. Vitic.* **52** 165–74 Online: https://www.ajevonline.org/content/ajev/52/3/165.full.pdf
30. Joos F, Bruno M, Fink R, Siegenthaler U, Stocker T, LeQuere C and Sarmiento J L 1996 An efficient and accurate representation of complex oceanic and biospheric models of anthropogenic carbon uptake *Tellus* **48B** 397–417
31. Kaplan J O, Prentice I C and Buchmann N 2002 The stable carbon isotope composition of the terrestrial biosphere: Modeling at scales from the leaf to the globe *Global Biogeochem. Cycles* **16** Online: %3CGo
32. Kay J E, Deser C, Phillips A, Mai A, Hannay C, Strand G, Arblaster J M, Bates S C, Danabasoglu G, Edwards J, Holland M, Kushner P, Lamarque J F, Lawrence D, Lindsay K, Middleton A, Munoz E, Neale R, Oleson K, Polvani L and Vertenstein M 2014 The Community Earth System Model (CESM) Large Ensemble Project: A Community Resource for Studying Climate Change in the Presence of Internal Climate Variability *Bull. Am. Meteorol. Soc.* Online: http://dx.doi.org/10.1175/BAMS-D-13-00255.1
33. Kennedy M C and O'Hagan A 2000 Predicting the output from a complex computer code when fast approximations are available *Biometrika* **87** 1–13 Online: papers2://publication/uuid/1A69EB40-F7E9-48E1-B609-FF3A7497DBC2
34. Klein Goldewijk K, Beusen A, Van Drecht G and De Vos M 2011 The HYDE 3.1 spatially explicit database of human-induced global land-use change over the past 12,000 years *Glob. Ecol. Biogeogr.* **20** 73–86
35. Lavigne F, Degeai J-P, Komorowski J-C, Guillet S, Robert V, Lahitte P, Oppenheimer C, Stoffel M, Vidal C M, Surono, Pratomo I, Wassmer P, Hajdas I, Hadmoko D S and de Belizal E 2013 Source of the great A.D. 1257 mystery eruption unveiled, Samalas volcano, Rinjani Volcanic Complex, Indonesia *Proc. Natl. Acad. Sci.* **110** 16742–7 Online: http://www.pnas.org/content/110/42/16742.abstract
36. van Leeuwen C and Darriet P 2016 The Impact of Climate Change on Viticulture and Wine Quality *J. Wine Econ.* **11** 150–67
37. Luterbacher J, Werner J P P, Smerdon J E E, Fernández-Donado L, González-Rouco F J J, Barriopedro D, Ljungqvist F C C, Büntgen U, Zorita E, Wagner S, Esper J, McCarroll D, Toreti A, Frank D, Jungclaus J H H, Barriendos M, Bertolin C, Bothe O, Brázdil R, Camuffo D, Dobrovolný P, Gagen M, García-Bustamante E, Ge Q, Gómez-Navarro J J J, Guiot J, Hao Z, Hegerl G C C, Holmgren K, Klimenko V V V, Martín-Chivelet J, Pfister C, Roberts N, Schindler A, Schurer A, Solomina O, Von Gunten L, Wahl E, Wanner H, Wetter O, Xoplaki E, Yuan N, Zanchettin D, Zhang H and Zerefos C 2016 European summer temperatures since Roman times *Environ. Res. Lett.* **11** 024001 Online: http://stacks.iop.org/1748-9326/11/i=2/a=024001?key=crossref.f0b0d73e9a56c730c57f879d45ca6bcb
38. Malheiro A C, Santos J A, Fraga H and Pinto J G 2010 Climate change scenarios applied to viticultural zoning in Europe *Clim. Res.* **43** 163–77
39. Mann M E, Fuentes J D and Rutherford S 2012 Underestimation of volcanic cooling in tree-ring-based reconstructions of hemispheric temperatures *Nat. Geosci.* **5** 202–5 Online: http://dx.doi.org/10.1038/ngeo1394
40. Mccormick M, Büntgen U, Cane M A, Cook E R, Harper K, Huybers P, Litt T, Manning S W, Mayewski P A, More A F M, Nicolussi K and Tegel W 2012 Climate Change During & After the Roman Empire *J. Interdiscip. Hist.* **xliii** 169–220
41. Moriondo M, Trombi G, Ferrise R, Brandani G, Dibari C, Ammann C M, Lippi M M and Bindi M 2013 Olive trees as bio-indicators of climate evolution in the Mediterranean Basin *Glob. Ecol. Biogeogr.* **22**
42. Muscheler R, Joos F, Beer J, Müller S A, Vonmoos M and Snowball I 2007 Solar activity during the last 1000yr inferred from radionuclide records *Quat. Sci. Rev.* **26** 82–97 Online: http://www.sciencedirect.com/science/article/pii/S0277379106002460

43. Myhre G, Shindell D, Bréon F-M, Collins W, Fuglestvedt J, Huang J, Koch D, Lamarque J-F, Lee D, Mendoza B, Nakajima T, Robock A, Stephens G, Takemura T and Zhang H 2013 Anthropogenic and Natural Radiative Forcing *Climate Change 2013: The Physical Science Basis. Contribution of Working Group I to the Fifth Assessment Report of the Intergovernmental Panel on Climate Change* ed T F Stocker, D Qin, G-K Plattner, M Tignor, S K Allen, J Boschung, A Nauels, Y Xia, V Bex and P M Midgley (Cambridge, United Kingdom and New York, NY, USA: Cambridge University Press) pp 659–740 Online: www.climatechange2013.org
44. Reale O and Dirmeyer P 2000 Modeling the effects of vegetation on Mediterranean climate during the Roman Classical Period. Part I: Climate history and model sensitivity *Glob. Planet. Change* **25** 163–84
45. Reale O and Shukla J 2000 Modeling the effects of vegetation on Mediterranean climate during the Roman Classical Period: Part II. Model simulation *Glob. Planet. Change* **25** 185–214
46. Rougier J and Goldstein M 2014 Climate Simulators and Climate Projections *Annu. Rev. Stat. Its Appl.* **1** 103–23 Online: http://www.annualreviews.org/doi/abs/10.1146/annurev-statistics-022513-115652
47. Le Roy Ladurie E, Daux V and Luterbacher J 2006 Vignes et vendanges des XIV-XXIe siècles *Hist. économie société* **25e année** 421–36 Online: https://www.cairn.info/load_pdf.php?ID_ARTICLE=HES_063_0421
48. Santos J A, Malheiro A C, Pinto J G and Jones G V. 2012 Macroclimate and viticultural zoning in Europe: Observed trends and atmospheric forcing *Clim. Res.* **51** 89–103
49. Sigl M, Winstrup M, McConnell J R, Welten K C, Plunkett G, Ludlow F, Büntgen U, Caffee M, Chellman N, Dahl-Jensen D, Fischer H, Kipfstuhl S, Kostick C, Maselli O J, Mekhaldi F, Mulvaney R, Muscheler R, Pasteris D R, Pilcher J R, Salzer M, Schüpbach S, Steffensen J P, Vinther B M and Woodruff T E 2015 Timing and climate forcing of volcanic eruptions for the past 2,500 years. *Nature* **523** 543–9 Online: http://www.ncbi.nlm.nih.gov/pubmed/26153860
50. Stoffel M, Khodri M, Corona C, Guillet S, Poulain V, Bekki S, Guiot J, Luckman B H, Oppenheimer C, Lebas N, Beniston M and Masson-Delmotte V 2015 Estimates of volcanic-induced cooling in the Northern Hemisphere over the past 1,500 years *Nat. Geosci.* **8** 784–8 Online: http://www.nature.com/doifinder/10.1038/ngeo2526
51. Strassmann K M and Joos F 2018 The Bern Simple Climate Model (BernSCM) v1.0: An extensible and fully documented open-source re-implementation of the Bern reduced-form model for global carbon cycle-climate simulations *Geosci. Model Dev.* **11** 1887–908
52. Terral J-F, Tabard E, Bouby L, Ivorra S, Pastor T, Figueiral I, Picq S, Chevance J-B, Jung C, Fabre L, Tardy C, Compan M, Bacilieri R, Lacombe T and This P 2010 Evolution and history of grapevine (Vitis vinifera) under domestication: new morphometric perspectives to understand seed domestication syndrome and reveal origins of ancient European cultivars *Ann. Bot.* **105** 443–55 Online: www.aob.oxfordjournals.org
53. Tonietto J and Carbonneau A 2004 A multicriteria climatic classification system for grape-growing regions worldwide *Agric. For. Meteorol.* **124** 81–97
54. Tran G T, Oliver K I C, Sóbester A, Toal D J J, Holden P B, Marsh R, Challenor P and Edwards N R 2016 Building a traceable climate model hierarchy with multi-level emulators *Adv. Stat. Climatol. Meteorol. Oceanogr.* **2** 17–37 Online: http://www.adv-stat-clim-meteorol-oceanogr.net/2/17/2016/
55. van Vuuren D P, Isaac M, Kundzewicz Z W, Arnell N, Barker T, Criqui P, Berkhout F, Hilderink H, Hinkel J, Hof A, Kitous A, Kram T, Mechler R and Scrieciu S 2011 The use of scenarios as the basis for combined assessment of climate change mitigation and adaptation *Glob. Environ. Chang.* **21** 575–91
56. Wanner H, Beer J, Bütikofer J, Crowley T J, Cubasch U, Flückiger J, Goosse H, Grosjean M, Joos F, Kaplan J O, Küttel M, Müller S A, Prentice I C, Solomina O, Stocker T F, Tarasov P, Wagner M and Widmann M 2008 Mid- to Late Holocene climate change: an overview *Quat. Sci. Rev.* **27** 1791–828
57. Warszawski L, Frieler K, Huber V, Piontek F, Serdeczny O and Schewe J 2014 The Inter-Sectoral Impact Model Intercomparison Project (ISI-MIP): project framework. *Proc. Natl. Acad. Sci. U. S. A.* **111** 3228–32
58. Zhu Q, Peng C, Chen H, Fang X, Liu J, Jiang H, Yang Y and Yang G 2015 Estimating global natural wetland methane emissions using process modelling: Spatio-temporal patterns and contributions to atmospheric methane fluctuations *Glob. Ecol. Biogeogr.* **24** 959–72

Tables

Table 1. Typical past periods used to calibrate our emulator. The paleoclimatic and societal information are found in the literature given in the references, from the Late Holocene to the Present.

Time slices and labels	Location	Climate	Societal events	References
4200 (4200-3900 yr BP)	The Levant, Mesopotamia, Sicily	Drought	Collapse of Akkadian empire in Mesopotamia	(*8*, *81*, *82*)
3200 (3300-2900 yr BP)	The Levant, Anatolia, Aegean, Egypt	Drought	Collapse/decline of Aegean, Hittite, Palestinian, Egyptian, Babylonian civilizations	(*6*, *83*)
	Mesopotamia			(*84*)
2500 (2600-2400 yr BP)	West Med, France	Cold	Early Iron Age	(Finné et al., 2011; Magny et al., 2013)
	the Maghreb	Dry		(*85*)
2000 (2100-1800 yr BP)	West Med, France, the Maghreb	Warm, wet	Roman Climate Optimum (RCO), expansion of the empire	(*1*, *21*)
1300 (1410-1290 yr BP or 536-660AD)	West Med, Alps	Cold	Late Antique Little Ice Age (LALIA) (migrations, pandemics, social turmoil)	(*21*)
	Mesopotamia, Iran	Dry	Demise of Sasanians	(*87*)
1000 (1150-650 yr BP or 800-1300AD)	Europe, Alps,	Warm	Medieval climate anomaly (MCA)	(*88*)(*89*)
	East	dry		(*86*, *90*)
700 (700-600 yr BP or 1250-1350 AD)	Europe, Alps	Cold	Beginning of Little Ice Age (LIA); famine, black death	(*30*, *89*)
200 (300-230 yr BP or 1650-1720)	Europe, Alps	Cold wet	Max of Little Ice Age (LIA); famines	(*82*, *89*)
	Spain	Dry		(*82*)
Present (1961-1990)		Warm and dry		CRU data (Jones et al, 2012)

Table 2. Forcing variables used for the 15 time slices/scenarios. The forcing greenhouse gas atmospheric concentrations (CO_2, CH_4, N_2O), orbital parameters (ecc: eccentricity, Obl: obliquity, Omega), population size (POP) in number of people, volcanic activity with uncertainty (d), solar activity with uncertainty (d).

Period	CO2	CH4	N2O	Ecc	Obl	Omega	POP	Volc [delta]	Sol [delta]
4200	280	650	270	0.0181	23.9	34	64138	0.2 [0.2]	200 [200]
3200	280	650	270	0.0178	23.8	45	101664	0.2 [0.2]	200 [200]
2500	280	650	270	0.0175	23.75	65	146283	0.6 [0.2]	270 [200]
2000	280	650	270	0.0175	23.7	68	188239	0.2 [0.2]	400 [300]
1300	280	650	270	0.0174	23.65	75	218535	0.6 [0.2]	270 [200]
1000	280	650	270	0.0173	23.65	75	295040	0.2 [0.2]	400 [300]
700	280	650	270	0.0175	23.5	90	396811	0.6 [0.2]	270 [200]
200	280	650	270	0.0169	23.4	95	813664	0.6 [0.2]	270 [200]
Present	400	1730	330	0.0167	23.45	102	7500000	0.2 [0.2]	600 [300]
+1.5C	440	1527	339	0.0167	23.45	102	8200000	0.2 [0.2]	270 [200]
+2C	487	1833	350	0.0167	23.45	102	8200000	0.2 [0.2]	270 [200]
+3C	603	3076	381	0.0167	23.45	102	8200000	0.2 [0.2]	270 [200]
+5C	900	3700	430	0.0167	23.45	102	12300000	0.2 [0.2]	270 [200]
5CV+	900	3700	430	0.0167	23.45	102	12300000	0.8 [0.2]	100 [200]
5CV-	900	3700	430	0.0167	23.45	102	12300000	0.1 [0.2]	700 [200]

Table 3. Posterior distribution of the parameters. The estimates are given by the best fit and the CI is the 90% confidence intervals calculated on the 10% best fits. Volc index has no units, Solar index is in MeV, T in °C, P, in mm/year.

	Volc	Volc.CI	Solar	Solar.CI	δT	δT.CI	σT	σT.CI	δP	δP.CI	σP	σP.CI
4200	0.1	[0.1, 0.27]	270	[153, 387]	0.3	[-1.7,1.7]	0.8	[0.4,4.7]	-15	[-19,3]	81	[70,81]
3200	0.15	[0.1, 0.33]	267	[190, 387]	-1	[-1.7,1.7]	2.6	[0.4,4.7]	-20	[-20,-7]	81	[66,81]
2500	0.4	[0.4, 0.75]	304	[103, 444]	0.6	[0.2,0.9]	2.1	[1.8,3.5]	16	[-17,18]	25	[5,77]
2000	0.17	[0.1, 0.38]	106	[106, 642]	1.6	[1.1,1.9]	0.9	[0.9,2.8]	-15	[-18,18]	53	[5,75]
1300	0.4	[0.4, 0.76]	324	[121, 452]	1	[0.5,1.3]	1.1	[1.1,2.9]	-9	[-18,18]	45	[6,76]
1000	0.22	[0.1, 0.39]	141	[141, 660]	1.3	[0.9,1.7]	0.9	[0.9,2.7]	-3	[-18,17]	6	[6,76]
700	0.62	[0.4, 0.78]	468	[109, 468]	1.2	[0.8,1.6]	0.9	[0.9,2.7]	-5	[-18,17]	25	[5,76]
200	0.41	[0.4, 0.77]	450	[97, 458]	1.2	[0.7,1.5]	0.3	[0.3,2.6]	4	[-18,17]	49	[5,76]
Present	0.36	[0.15, 0.4]	345	[307, 548]	0.7	[-0.3,1.6]	0.3	[0.2,4.6]	-14	[-18.7,10]	57	[36,79]

Figures

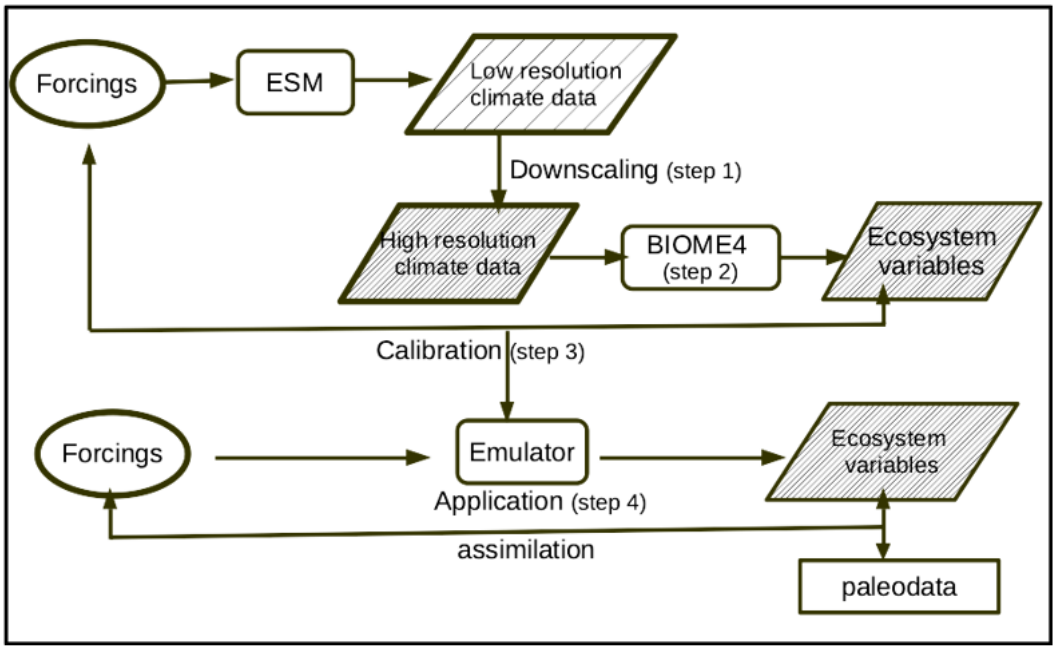

Figure 1

Diagram of the different steps in the emulator approach; the ecosystem variables, related to bioclimate and net primary productivity, are defined in Table S1.

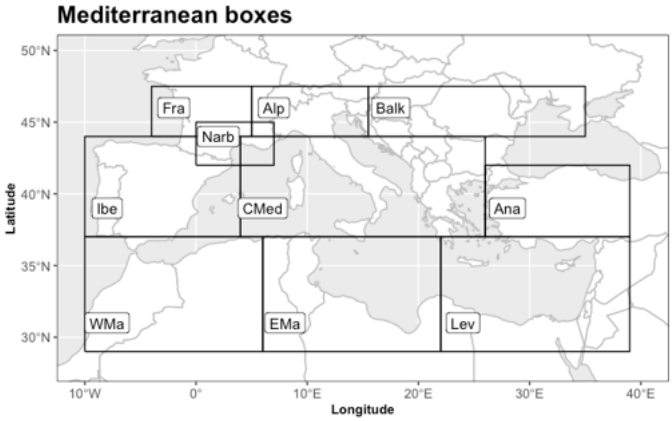

Figure 2

Map of the 10 boxes defined in the Mediterranean region.

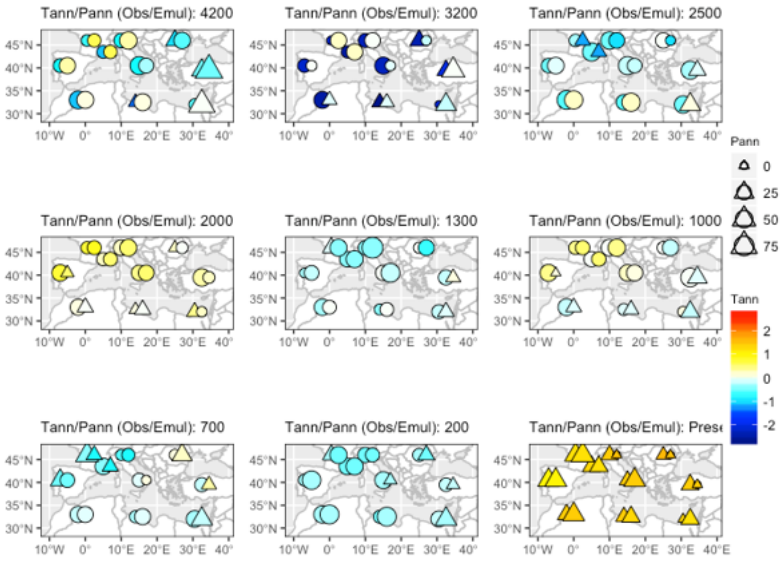

Figure 3

Spatial distribution of the temperature and precipitation anomalies for the past and present time slices. The pairs of symbols are simulations (left symbols) and observations or pollen reconstructions (right symbols). The colors are used for the temperature anomalies. Triangles are used for negative precipitation anomalies and circles for the positive precipitation anomalies. The size of the triangles and circles is proportional to the absolute value of the anomalies.

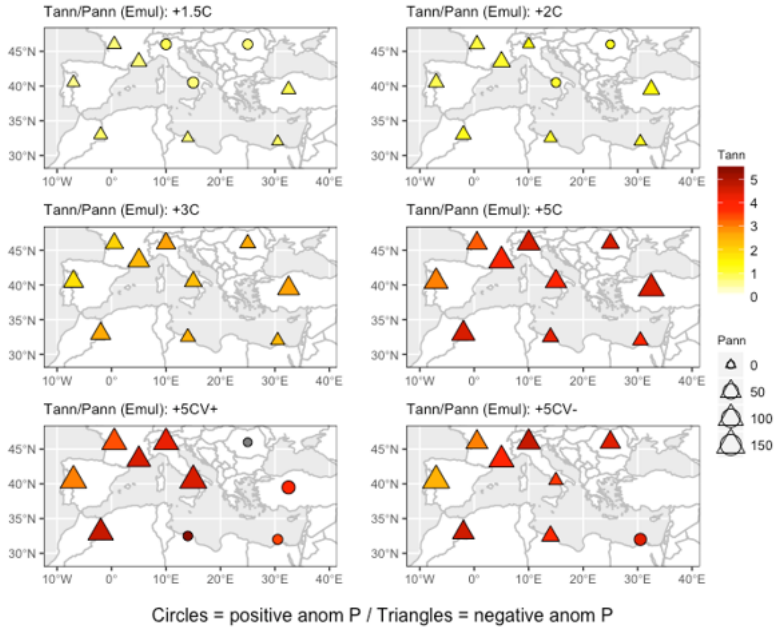

Figure 4

Spatial distribution of the temperature and precipitation anomalies simulated for future time slices (scenarios). The colors are used for the temperature anomalies. Triangles are used for negative precipitation anomalies and circles for positive precipitation anomalies. The size of the triangles and circles is proportional to the absolute value of the anomalies.

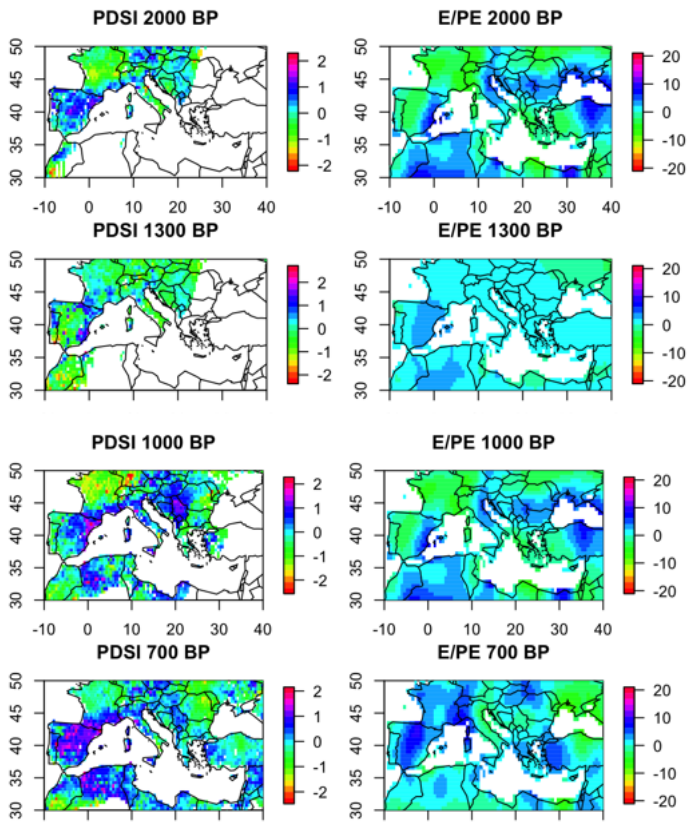

Figure 5

Comparison of E/PE reconstructed in this paper with independently reconstructed PDSI. The PDSI anomalies are based on the 1928-1978 reference period, and are reconstructed from tree rings (*45*). E/PE is the ratio of actual to potential evapotranspiration obtained from the emulator (in %).

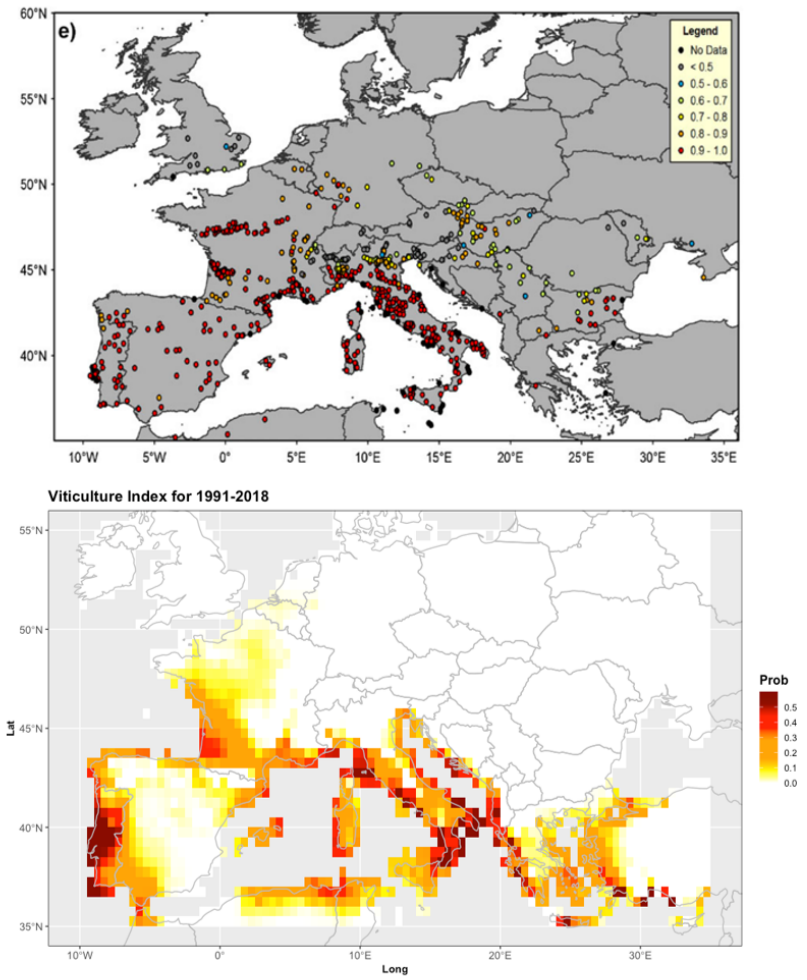

Figure 6

Distribution of the wine sites: (a) European wine regions (circles) with the corresponding CompI value for the period of 1980–2009, Fig 1e of Fraga et al. (*49*). (b) Simulation using the viticulture index calculated using 1961-1990 climate data.

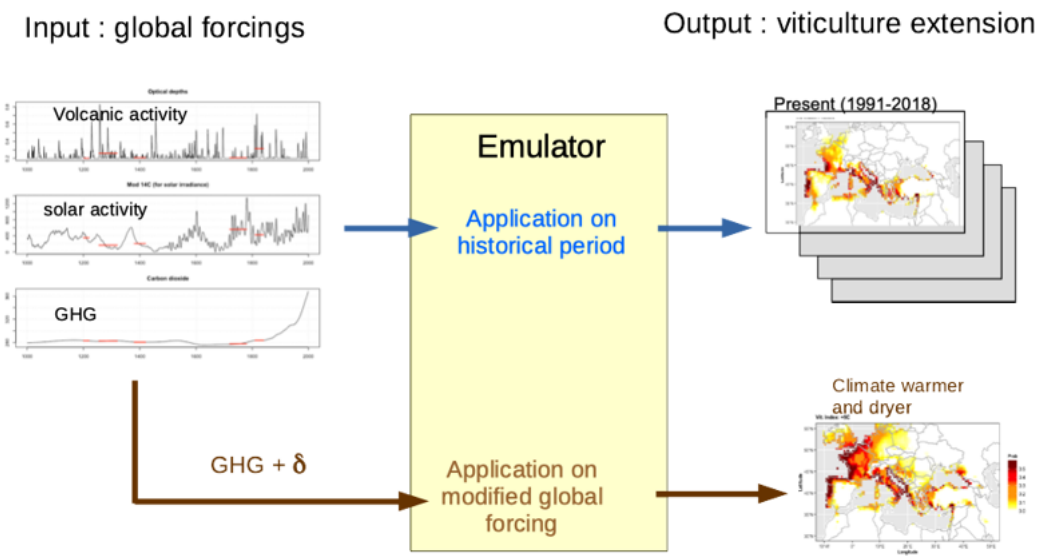

Figure 7

Diagram of the application of the emulator to reconstruct and predict the viticulture extension

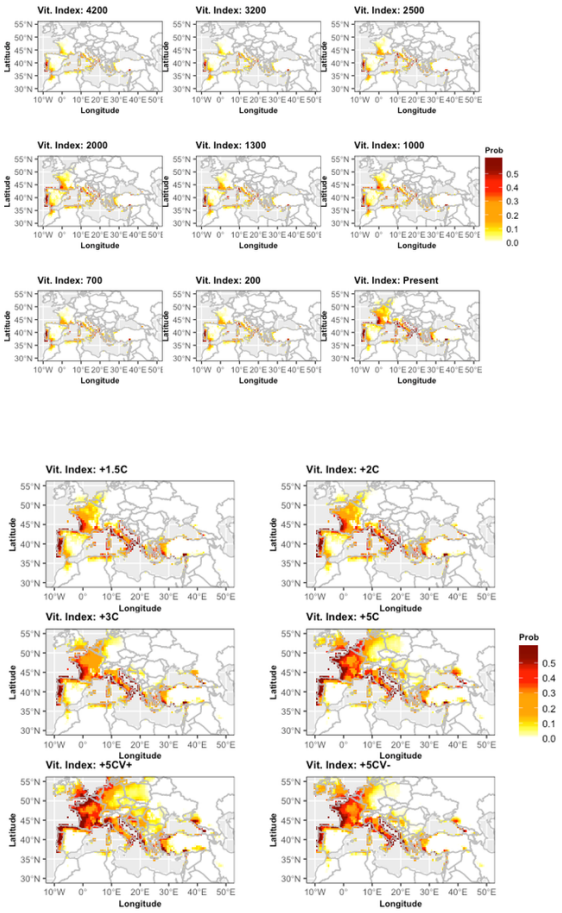

Figure 8

Distribution of the viticulture index (Vit. Index) for several time slices of the past (in yr BP) and future scenarios (expressed as anomalies of global temperature vs pre-industrial reference). The index is labelled VI and is explained in eq.1. White areas indicate where it is impossible to cultivate vine.

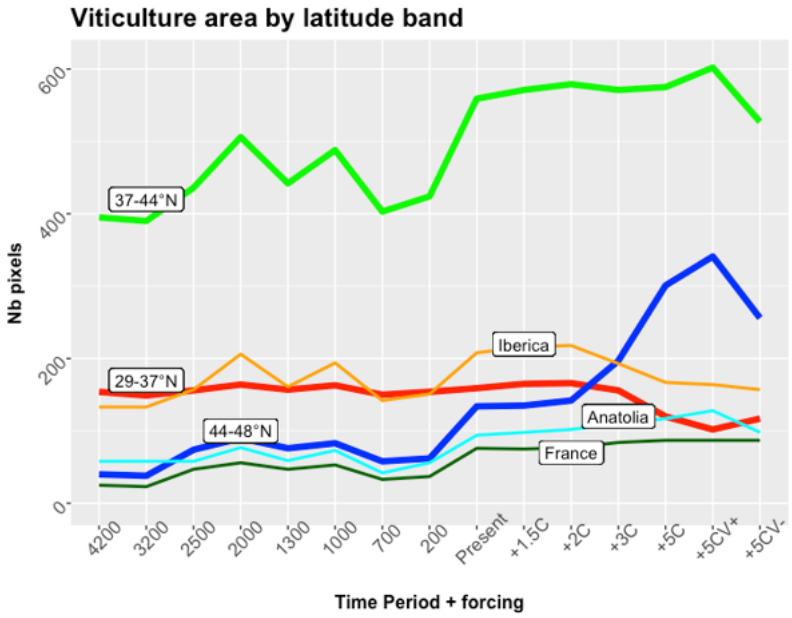

Figure 9

Synthesis of the evolution of viticulture in the Mediterranean area. The curves represent three bands of latitude: southern band with latitude<37°N in red, center band with latitudes between 37 and 44°N in green, northern band with latitudes between 44 and 48°N in blue). The thin lines show the results for the boxes corresponding to Iberian Peninsula, Anatolia and France (definition in Fig. 1). The scenarios and time slices are defined in Table 2 plus the two additional scenarios (+5CV+, +5CV-) explained in the text. The x-axis gives the center of the time slices considered or the future scenario.

Supplementary Files

This is a list of supplementary files associated with this preprint. Click to download.

- ViticultureforcingsMedCCSMv2.docx